THE JOURNAL OF BIOLOGICAL CHEMISTRY VOL. 287, NO. 53, pp. 44645–44653, December 28, 2012

Sphingosine 1-Phosphate (S1P) Carrier-dependent Regulation of Endothelial Barrier

HIGH DENSITY LIPOPROTEIN (HDL)-S1P PROLONGS ENDOTHELIAL BARRIER ENHANCEMENT AS COMPARED WITH ALBUMIN-S1P VIA EFFECTS ON LEVELS, TRAFFICKING, AND SIGNALING OF S1P1[*][S]

Received for publication, September 27, 2012 Published, JBC Papers in Press, November 7, 2012, DOI 10.1074/jbc.M112.423426

Brent A. Wilkerson[1], **G. Daniel Grass**[2], **Shane B. Wing, W. Scott Argraves, and Kelley M. Argraves**[3]

From the Department of Regenerative Medicine and Cell Biology, Medical University of South Carolina, Charleston, South Carolina 29425

Background: S1P promotes endothelial barrier and is associated with HDL and albumin in blood.
Results: HDL-S1P sustained barrier longer than albumin-S1P, reduced S1P receptor (S1P1) degradation, increased S1P1 cell surface and lipid raft levels, and persistently activated PI3K-Akt and eNOS.
Conclusion: HDL-S1P persistently activates S1P-S1P1-PI3K-Akt-eNOS signaling.
Significance: The findings highlight the basis for HDL-S1P as a mediator of sustained endothelial barrier.

Sphingosine 1-phosphate (S1P) is a blood-borne lysosphingolipid that acts to promote endothelial cell (EC) barrier function. In plasma, S1P is associated with both high density lipoproteins (HDL) and albumin, but it is not known whether the carriers impart different effects on S1P signaling. Here we establish that HDL-S1P sustains EC barrier longer than albumin-S1P. We showed that the sustained barrier effects of HDL-S1P are dependent on signaling by the S1P receptor, S1P1, and involve persistent activation of Akt and endothelial NOS (eNOS), as well as activity of the downstream NO target, soluble guanylate cyclase (sGC). Total S1P1 protein levels were found to be higher in response to HDL-S1P treatment as compared with albumin-S1P, and this effect was not associated with increased S1P1 mRNA or dependent on *de novo* protein synthesis. Several pieces of evidence indicate that long term EC barrier enhancement activity of HDL-S1P is due to specific effects on S1P1 trafficking. First, the rate of S1P1 degradation, which is proteasome-mediated, was slower in HDL-S1P-treated cells as compared with cells treated with albumin-S1P. Second, the long term barrier-promoting effects of HDL-S1P were abrogated by treatment with the recycling blocker, monensin. Finally, cell surface levels of S1P1 and levels of S1P1 in caveolin-enriched microdomains were higher after treatment with HDL-S1P as compared with albumin-S1P. Together, the findings reveal S1P carrier-specific effects on S1P1 and point to HDL as the physiological mediator of sustained S1P1-PI3K-Akt-eNOS-sGC-dependent EC barrier function.

A major physiological function of the vascular endothelium is to act as a selective barrier, regulating the exchange of liquids and solutes and the passage of cells (1). This critical role is evident in various pathological processes that cause increased vascular permeability including hypertension and stroke, myocardial infarction, ischemia-reperfusion, acute lung injury, sepsis, inflammatory disorders, tumor invasion, diabetic retinopathy, and macular edema (2, 3).

Sphingosine 1-phosphate (S1P)[4] is a blood-borne lysosphingolipid that acts to enhance the barrier function of the vascular endothelium (4, 5). Considering the importance of vascular barrier regulation in physiology and disease, defining the mechanisms by which S1P enhances integrity of the endothelial cell barrier is an area of active research (6–12).

In blood, S1P is associated predominantly with apolipoprotein M (apoM)-containing HDL and to a lesser extent with albumin (13, 14). However, most studies of S1P bioactivity have employed albumin as the S1P carrier, thus raising questions whether the observed effects of albumin-S1P can be extended to HDL-S1P and whether there are carrier-specific effects on S1P signaling. Here we evaluate the influence of albumin-S1P and HDL-S1P on endothelial cell barrier function and discover that the two have distinct effects on the persistence of S1P-dependent barrier enhancement that relate to differential effects on the trafficking and stabilization of the S1P receptor, S1P1, and its signaling.

EXPERIMENTAL PROCEDURES

Culture of Human Umbilical Vein Endothelial Cells—Human umbilical vein endothelial cells (HUVECs, Cascade Bio-

* This work was supported, in whole or in part, by National Institutes of Health Grants HL094883 and HL080404 (to K. M. A.) and HL061873 (to W. S. A.).
[S] This article contains supplemental Table 1 and Figs. 1–4.
[1] Supported by National Institutes of Health Training Grant T32HL007260 and by a fellowship from the American Heart Association (Grant 10PRE3910006).
[2] Supported by a United States Department of Defense predoctoral fellowship (Grant W81XWH-10-1-0083).
[3] To whom correspondence should be addressed: Dept. of Regenerative Medicine and Cell Biology, Medical University of South Carolina, 173 Ashley Ave., Charleston, SC 29425-2204. Tel.: 843-792-3535; Fax: 843-792-0664; E-mail: argravek@musc.edu.

[4] The abbreviations used are: S1P, sphingosine 1-phosphate; EC, endothelial cell; HUVEC, human umbilical vein endothelial cell; TEER, trans-endothelial electrical resistance; ECIS, electric cell-substrate impedance sensing; apoM, apolipoprotein M; CEM, caveolin-enriched microdomain; eNOS, endothelial NOS; sGC, soluble guanylate cyclase; EBM, endothelial basal medium-2; DMSO, dimethyl sulfoxide; ANOVA, analysis of variance; ODQ, 1*H*-[1,2,4]oxadiazolo[4,3-a]quinoxalin-1-one; L-NAME, *N*-nitro-L-arginine methyl ester.

logics, Inc.) were maintained in humidified 5% CO_2, 95% air in endothelial growth medium-2 (Lonza; Basel, Switzerland), containing 2% fetal bovine serum. Serum starvation and experiments measuring S1P responses were carried out in serum-free endothelial basal medium-2 (EBM) (Lonza) with 0.5× penicillin streptomycin glutamine (Invitrogen) and 0.5× GlutaMAX (Invitrogen). Unless specified otherwise, experimentation described in the present studies used confluent passage 2–5 HUVEC monolayers serum-starved 48 h.

Reagents—S1P (D-erythro-S1P) was purchased from Avanti Polar Lipids, Inc. (Alabaster, AL). The S1P1 antagonist W146 was purchased from Avanti Polar Lipids and dissolved in acidified dimethyl sulfoxide (DMSO), 4 mg/ml fatty acid-free bovine serum albumin (BSA). The protein synthesis inhibitor cycloheximide was obtained from Sigma-Aldrich and dissolved in DMSO. The recycling inhibitor monensin was purchased from Sigma-Aldrich and dissolved in methanol. The PI3K inhibitor LY294002 was purchased from R&D Systems, Inc. (Minneapolis, MN) and dissolved in DMSO. The endothelial NOS (eNOS) inhibitor L-NAME was purchased from Alexis Biochemicals (San Diego, CA) and dissolved in serum-free EBM. The inhibitor of soluble guanylate cyclase 1*H*-[1,2,4]oxadiazolo[4,3-a]quinoxalin-1-one (ODQ) was purchased from Cayman Chemical (Ann Arbor, MI) and dissolved in DMSO.

Reconstitution of S1P in Albumin and Quantification of S1P—100 μM stock solutions of S1P were prepared fresh daily by dissolving S1P into Dulbecco's PBS (PBS) containing 4 mg/ml fatty acid-free BSA. Measurement of S1P levels in stock albumin-S1P solutions and HDL was performed by the Lipidomics Core Facility at the Medical University of South Carolina using LC-MS-MS methods for detection of S1P with subpicomolar sensitivity (15).

Purification of HDL—HDL (1.063–1.21 g/ml) was purified by density gradient ultracentrifugation of EDTA-plasma (16), typically collected from 2–3 healthy, normolipidemic donors. HDL fractions were dialyzed against a PBS, 0.03 mM EDTA solution (HDL storage buffer). Protein levels of HDL preparations were determined by Bio-Rad DC protein assay (Bio-Rad).

S1P Fortification of HDL—In some cases, purified HDL was fortified with exogenous S1P to bolster S1P concentrations to physiological levels. S1P fortification of HDL was achieved by incubating HDL with lyophilized S1P in HDL storage buffer followed by dialysis against HDL storage buffer. S1P and protein contents of the resulting HDL preparations were determined by LC-MS-MS and Bio-Rad DC protein assay, respectively. In all cases, findings made using fortified HDL were similar to those obtained using native, unaltered HDL.

Trans-endothelial Electrical Resistance Measurement and Analysis—Endothelial barrier integrity was measured in real time as trans-endothelial electrical resistance (TEER). TEER of confluent monolayers of HUVECs was measured using an Applied Biophysics ECIS 1600 instrument (Applied Biophysics, Troy, NY) as described previously (9). Cells were seeded at a density of 1.5×10^5 cells/well onto 8W10E+ electric cell-substrate impedance sensing (ECIS) arrays (Applied Biophysics) coated with human plasma fibronectin (Invitrogen) at 100 μg/ml in 0.15 M NaCl, 0.01 M Tris, pH 8.0. Cells were cultured to confluence until electrical impedance reached a maximal plateau (~1400–1600 ohms, ~48 h). The medium was then replaced with serum-free EBM, resulting in a drop in impedance. When impedance reached a minimum plateau (~800–1000 ohms, 24–48 h), effectors (*e.g.* HDL-S1P) were added to culture medium, and the TEER response was measured for up to 20 h. The maximum volume of each effector added did not exceed one-tenth of the 400-μl volume of culture medium in each well. In studies evaluating specific effectors, controls included treatments with matched volumes of fatty acid-free serum albumin, HDL storage buffer, or vehicle buffers.

ECIS impedance values were first normalized by dividing each value by the level of impedance measured just prior to the addition of effectors. To quantify differences in barrier activity in response to effectors, the area under the normalized impedance traces was calculated in KaleidaGraph Version 4.0.3 (Synergy Software, Reading, PA) using the "Integrate-Area" macro. Integrated impendence values for effectors (*e.g.* albumin-S1P or HDL-S1P) were divided by integrated mean impendence values for control agents (*e.g.* S1P free albumin in PBS) for the specified period of time.

Phospho-Akt, Phospho-ERK1/2, and Phospho-eNOS Detection—Bio-Plex phospho-Akt and phospho-ERK1/2 detection was carried out as described previously (9). To detect phospho-eNOS, cells were extracted in lysis buffer (1% Nonidet P-40, 20 mM Tris, 137 mM NaCl, and Roche Applied Science Minitab protease inhibitor mixture) plus 100 nM okadaic acid, and the extracts were subjected to immunoblot analysis using antibodies to phospho-eNOS (serine 1177) and eNOS (BD Pharmingen).

S1P1 Immunoblot Analysis—HUVECs were seeded into 6-well plates (Corning, Lowell, MA) at $1.5–3 \times 10^5$ cells/well and grown to confluence. The medium was then replaced with serum-free EBM. After 48 h of serum starvation, HDL or albumin containing equal molar amounts of S1P was added to culture medium (control wells received equal volumes of S1P-free vehicle). HUVECs were lysed in 200 μl of ice-cold lysis buffer. Lysates were subjected to centrifugation at 7500 × *g* for 10 min at 4 °C, and protein levels in the supernatants were measured using the Bio-Rad DC protein assay. Aliquots were subjected to SDS-PAGE and transferred to PVDF membranes (Santa Cruz Biotechnology, Inc.; Santa Cruz, CA). Membranes were blocked in TBS, pH 7.4, containing 5% milk and incubated with rabbit anti-human S1P1 (H-60) (sc-25489; Santa Cruz Biotechnology) in TBS, 0.1% Tween 20 overnight at 4 °C. After washing, the membranes were incubated with horseradish peroxidase-conjugated donkey anti-rabbit IgG secondary antibody (Jackson ImmunoResearch Laboratories, West Grove, PA) in TBS, 0.1% Tween 20. Detection was achieved using Amersham Biosciences ECL Plus reagents (GE Healthcare). To control for protein loading, blots were probed using rabbit anti-human cytochrome oxidase-IV (AB16056; Abcam, Cambridge, MA), actin (A2668, Sigma), or GAPDH (AB37168, Abcam).

Cell Surface S1P1 Analysis—HUVECs were grown to confluence in 100-mm plates and then serum-starved 48 h. Following the indicated treatments, HUVEC surface proteins were isolated using the Pierce cell surface protein isolation kit (Pierce). Immunoblot analysis was performed on the cell surface fractions using antibodies to S1P1 (Santa Cruz Biotechnology) and

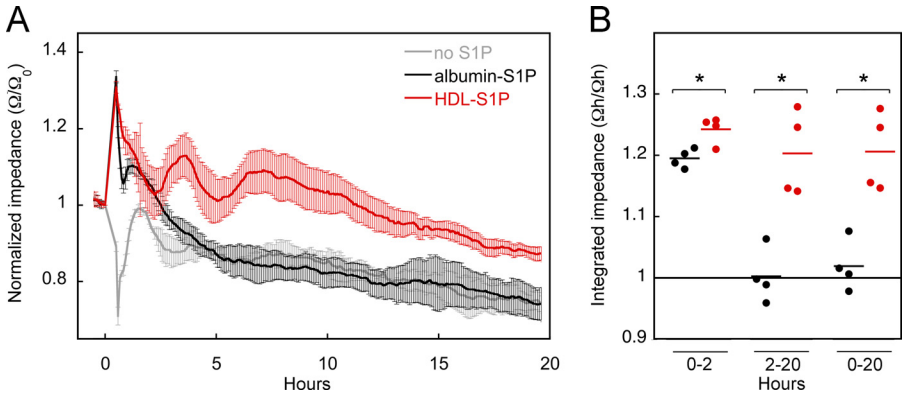

FIGURE 1. **HDL-S1P sustains endothelial barrier activity longer than albumin-S1P.** Endothelial cells were treated with HDL-S1P, albumin-S1P (each containing 150 nM S1P), or S1P-free vehicle (*no S1P*). In *A*, each of the TEER tracings is an average from four replicate wells. Wells treated with HDL-S1P received fatty acid-free serum albumin, wells treated with albumin-S1P received HDL storage buffer, and control wells received matched volumes of fatty acid-free serum albumin and HDL storage buffer. Ω indicates ohms. *B* shows integrated impedance values (*i.e.* area under impedance traces), which are integrated impendence values for effectors divided by integrated mean impendence values for control agents for the specified period of time. Student's *t* test was used to test for significant differences in mean integrated impedance. *Asterisks* indicate $p < 0.01$.

rabbit anti-human von Willebrand factor (Dako, Carpentaria, CA); the latter was used to normalize for protein loading.

Analysis of S1P1 in Membrane Fractions Prepared by Discontinuous Gradient Ultracentrifugation—HUVECs were lysed (17), and the lysates were subjected to ultracentrifugation over discontinuous 0–40% OptiPrep gradients (18). 12 density fractions were collected, and aliquots were assayed by immunoblot using rabbit antibodies to S1P1 (Santa Cruz Biotechnology) and caveolin-1 (BD Pharmingen).

Immunofluorescent Labeling of S1P1—HUVECs were seeded in 4-well glass chamber slides (Nalge Nunc; Rochester, NY) and serum-starved 48 h. Following incubation with indicated effectors, cells were fixed for 20 min in 3% paraformaldehyde, washed in PBS, and permeabilized in PBS, 0.1% Triton-X-100, 0.01% azide for 30 min and then blocked in PBS containing 3% BSA and 5% donkey serum. Cultures were labeled with antibody to S1P1 and Alexa Fluor 488-conjugated donkey anti-rabbit secondary (Invitrogen). Nuclei were stained with Draq5 (5 μM; Axxora, San Diego, CA). Slides were analyzed using a Leica SP-5 confocal microscope system (Leica Microsystems Inc., Exton, PA). Analysis of micrographs contains data representative of at least five random fields. Immunofluorescence micrographs were collected using identical microscopy settings in a single session. Montages of primary images were adjusted equally using "Levels" in Photoshop. Background signal in empty, acellular space was subtracted using the black level slider. Brightness was increased using the white level slider to provide clarity of details in the original images. The gamma slider was not independently adjusted. "Rainbow RGB" look-up table was applied using ImageJ to demonstrate relative quantitative differences in the distribution of S1P1 immunofluorescence.

S1P1 mRNA Quantification by RT-PCR—RNA was isolated from HUVECs using RNA STAT-60 (Tel-Test, Inc., Friendswood, TX). Contaminating genomic DNA was digested by treatment with TURBO DNA-free DNase (Ambion, Inc., Austin, TX). Reverse transcription of total RNA was performed using reverse transcriptase and the SuperScript first-strand synthesis system containing random hexamers (Invitrogen). Oligonucleotide primers used for quantitative reverse transcriptase PCR are described in supplemental Table 1. Primers were designed using the computer programs mFold (19) and Primer3 (20). PCR was performed on a Bio-Rad iCycler using primer pairs (400 nM) together with template cDNAs and iQ SYBR Green supermix (Quanta Biosciences, Gaithersburg, MD). Cycling conditions used were 40 cycles of denaturation (95 °C for 30 s), annealing (60 °C for 30 s), and elongation (72 °C for 30 s). Controls were performed using RNA and cDNA synthesis reaction components minus reverse transcriptase. Real-Time PCR Miner was used for calculation of efficiency and fluorescence threshold crossing-cycle (C^T) values (21). Average C^T values and efficiencies of replicate reactions were normalized to the internal control gene GAPDH. Relative expression differences of S1P1 (fold difference) were calculated using the Pfaffl equation (22).

Plots and Statistical Analysis—Statistical tests and plots were done using KaleidaGraph. *Error bars* depict S.D. In dot plots, *bars* represent means. For comparison of one- or two-treatment groups, Student's *t*-tests were used with assumption of equal variance for unpaired data unless unequal variance was identified (*i.e.* *F* test, $p < 0.05$). Two-sided *p* values are reported except where it is otherwise indicated. In cases where three or more groups were compared, one-way ANOVA ($\alpha = 0.05$) and Tukey's pairwise tests were used. For ANOVA, two-sided *p* values are reported. *y* indicate $p < 0.05$.

RESULTS

HDL-S1P Sustains Endothelial Cell Barrier Function Longer than Albumin-S1P—TEER analysis was used to compare the endothelial barrier-enhancing activities of HDL and albumin, each containing equal molar amounts of S1P (150 nM). As shown in Fig. 1, within minutes of treatment, both albumin-S1P and HDL-S1P elicited increases in impedance, reaching similar maximal levels after ~30 min. Following this initial period, impedance levels in albumin-S1P-treated cultures steadily declined, reaching the level of S1P-free vehicle control at ~4 h (Fig. 1), whereas the level of impedance induced by HDL-S1P remained above the vehicle control base line for at least 20 h (Fig. 1*A*) and the difference was statistically significant over that period ($p = 0.003$; Fig. 1*B*). The inability of albumin-S1P to promote barrier after 4 h was not due to a reduction in S1P levels in the medium at later time points because LC-MS-MS

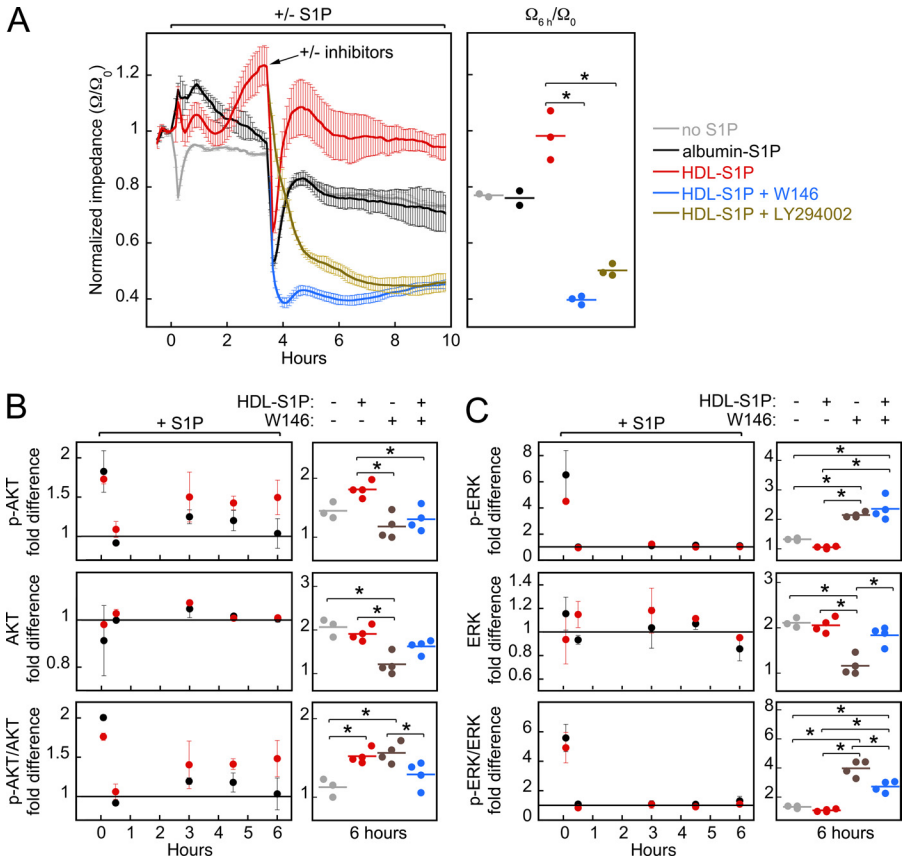

FIGURE 2. **HDL-S1P-sustained endothelial barrier activity is dependent on S1P1 signaling involving Akt activation.** *A* shows ECIS analysis of endothelial cells treated for ~4 h with HDL-S1P, albumin-S1P (each containing 150 nM S1P), or S1P-free vehicle (*no S1P*) followed by addition (*arrow*) of the S1P1 antagonist W146 (3.3 μM), the PI3K inhibitor LY294002 (50 nM), or vehicle. The *asterisks* indicate that the level of HDL-induced endothelial cell barrier is significantly reduced ($p < 0.0001$) 2 h following S1P1 antagonism as determined by one-way ANOVA and Tukey's post hoc test ($\alpha = 0.05$). The TEER tracings shown represent mean normalized impedance values of 2–3 replicate wells for each treatment. These results are representative of data from at least three independent experiments. Ω indicates ohms. *B* and *C*, show multiplex bead array analysis showing the temporal effects of albumin-S1P and HDL-S1P (150 nM S1P) treatments on the phosphorylation of Akt and ERK (*p-AKT* and *p-ERK*), respectively. *Left panels* show mean -fold changes in Akt/ERK ($n = 2$) at 5 min, 30 min, 3 h, 4.5 h, and 6 h relative to base-line Akt/ERK levels measured in S1P-free control treatments at each time point. *Right panels* show independent Akt/ERK assays 6 h after the indicated treatments each having 3–4 replicates. *Asterisks* indicate significant changes in Akt/ERK ($p < 0.05$) as determined by one-way ANOVA and Tukey's pairwise tests ($\alpha = 0.05$).

analysis of the culture medium from endothelial cells treated with either C17-S1P-fortified HDL or C17-S1P-fortified albumin showed no discernable reduction in S1P over the 6-h time course, irrespective of the carrier (supplemental Fig. 2*A*). Furthermore, exposure of the cells to HDL-S1P followed by washing the cell layer and replacement of the medium with HDL-S1P-free medium showed that HDL-S1P must be continuously present to achieve maximal barrier enhancement (supplemental Fig. 2*B*).

HDL-sustained Endothelial Cell Barrier Activity Is Dependent on S1P1 Signaling Involving Akt and eNOS Activation—Previous studies have established that HDL promotes endothelial barrier enhancement via S1P signaling dependent on the S1P1 receptor and components of the PI3K-Akt pathway (9). To determine whether the sustained endothelial barrier enhancement activity of HDL was mediated via the S1P-S1P1-PI3K-Akt signaling pathway, we first assessed the effect of the S1P1 antagonist, W146, on HDL-S1P-stimulated barrier occurring ~4 h following initiation of HDL-S1P treatment (*i.e.* the period of time at which albumin-S1P-induced barrier effects have waned). W146 was therefore added at 4 h following HDL-S1P treatment. As shown in Fig. 2*A*, S1P1 antagonism eliminated the sustained barrier effects of HDL-S1P.

We also evaluated the effect of the PI3K inhibitor, LY294002, on HDL-S1P-stimulated barrier occurring ~4 h following initiation of HDL-S1P treatment. PI3K inhibition completely reduced the level of HDL-induced barrier to levels below S1P-free vehicle treatments (Fig. 2*A*).

We next evaluated the level of Akt activation during the phase of HDL-S1P-stimulated barrier enhancement. At 4.5 and 6 h after treatment, HDL-S1P elevated phospho-Akt levels over those measured in response to either albumin-S1P or S1P free control treatments (Fig. 2*B*). By contrast, HDL-S1P treatment only elicited a short-lived effect (<30 min) on the activation Erk1/2, with no activation apparent in the 0.5–6-h window of observation as compared with S1P-free control (Fig. 2*C*). These findings emphasize that the sustained HDL-S1P barrier effects are dependent on PI3K-Akt activation. These studies also revealed that S1P1 inhibition reduced the levels of total Akt (Fig. 2*B*), suggesting that S1P1 signaling sustains Akt levels in addition to augmenting Akt activation.

Although HDL-S1P did not stimulate Erk1/2 activation at 6 h, S1P1 antagonist treatment augmented Erk1/2 activation at 6 h, suggesting that persistent HDL-S1P-S1P1 signaling might be eliciting a suppressive effect on Erk1/2 activation (Fig. 2*C*).

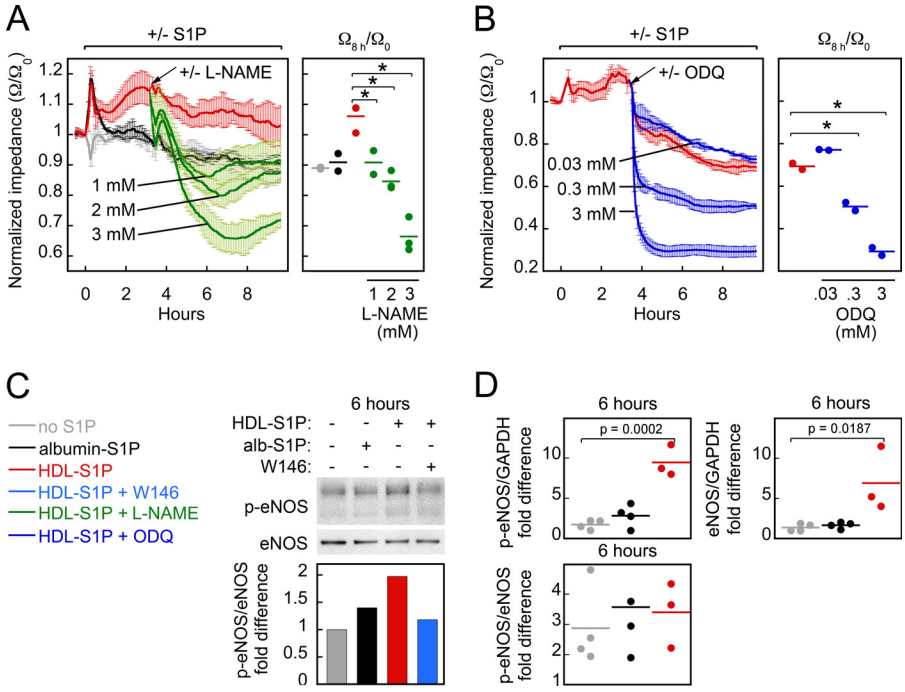

FIGURE 3. **HDL-S1P-sustained endothelial barrier activity is dependent on eNOS activity.** *A*, ECIS analysis of endothelial cells treated for 3 h with HDL-S1P, albumin-S1P (each containing 150 nM S1P), or S1P-free vehicle followed by the addition of the eNOS inhibitor L-NAME (1–3 mM) or vehicle (*arrow*). Each of the TEER tracings shown is an average of 2–3 replicates per condition and is representative of data from three independent experiments. Significant differences in normalized impedance at 8 h after S1P stimulation were identified by one-way ANOVA and Tukey's pairwise tests ($\alpha = 0.05$). *Asterisks* indicate $p < 0.038$. Ω indicates ohms. *B* and *C* show anti-eNOS and phospho-eNOS (*p-eNOS*) (phospho-serine 1177 eNOS) immunoblot analysis of endothelial cell extracts isolated 6 h after the addition of the indicated effectors. Plots in *B* and *C* show -fold differences in eNOS and phospho-eNOS protein levels as determined by densitometric analysis and normalized to GAPDH levels. Significant differences in phospho-eNOS and eNOS levels were identified by one-way ANOVA and Tukey's pairwise tests ($\alpha = 0.05$). *alb-S1P*, albumin-S1P. *D* shows an ECIS analysis of endothelial cells treated for 3 h with HDL-S1P (containing 150 nM S1P) followed by the addition of the sGC inhibitor ODQ (30–3000 nM) or vehicle (*arrow*). Each of the TEER tracings shown is an average of 2–3 replicates per condition and is representative of data from two independent experiments.

This is consistent with other findings showing that S1P-S1P1 signaling inhibits endothelial cell Erk1/2 activation through induction of MAP kinase phosphatase-3 (23). Our studies also revealed that S1P1 inhibition reduced the levels of total Erk1/2 and that HDL-S1P diminished this effect (Fig. 2*C*), indicating that S1P1 signaling sustains total Erk1/2 levels, while inhibiting activation at 6 h.

HDL-S1P signaling in endothelial cells also involves eNOS activation via phosphorylation of Ser-1177 (24). Active eNOS catalyzes production of nitric oxide (NO), a modulator of both vascular tone and endothelial barrier (25, 26). To determine whether eNOS activity was required for the sustained EC barrier-promoting effects of HDL-S1P, the eNOS/NO synthesis inhibitor, L-NAME, was used. L-NAME was found to cause dose-dependent inhibition of the sustained effects of HDL-S1P on EC barrier (Fig. 3*A*).

We next measured changes in phosphorylated eNOS and total eNOS in endothelial cells after 6 h of treatment with HDL-S1P or albumin-S1P. The results show that HDL-S1P, but not albumin-S1P, mediates prolonged Ser-1177 phosphorylation of eNOS for at least 6 h (Fig. 3, *C* and *D*, *left panel*). HDL-S1P-induced phosphorylation of eNOS at Ser-1177 was reduced by treatment with the S1P1 antagonist, W146 (Fig. 3*C*). In addition to augmenting eNOS activation, HDL-S1P treatment was also found to increase the levels of total eNOS (Fig. 3*D*, *right panel*), which is consistent with findings of others who showed that HDL promotes eNOS protein stability (27).

Because soluble guanylate cyclase (sGC) activation occurs in response NO and has been implicated in promoting barrier (28), we sought to determine whether sGC activity was required for the sustained EC barrier-promoting effects of HDL-S1P. We found that the sGC inhibitor, ODQ, elicited a dose-dependent inhibition of the sustained effects of HDL-S1P on EC barrier (Fig. 3*B*).

S1P1 Protein Levels Are Higher in Response to HDL-S1P as Compared with Albumin-S1P—We were next interested to determine whether the differential effects of HDL-S1P and albumin-S1P on S1P1-mediated barrier enhancement were reflective of alterations in S1P1 expression. In other studies, albumin-S1P induces time-dependent loss of S1P1 protein (29, 30). Using S1P1 immunoblot analysis, we observed that both albumin-S1P and HDL-S1P treatment elicited a time-dependent decrease in total S1P1 levels (Fig. 4*A*). However, in endothelial cells treated with HDL-S1P, there were higher levels of S1P1 protein at 2 and 6 h after treatment as compared with cells treated with albumin-S1P (Fig. 4*A*). In fact, levels of S1P1 were ~2-fold higher in endothelial cells treated with HDL-S1P as compared with albumin-S1P ($p = 0.0129$) at 6 h after treatment (Fig. 4*B*). Specificity of rabbit anti-S1P1 used for immunoblot analysis is shown in supplemental Fig. 1.

Effects of HDL-S1P on S1P1 Levels Are Not Due to Alterations in S1P1 Transcription or Protein Synthesis—Quantitative PCR analysis showed that the effect of HDL-S1P treatment on S1P1 protein levels did not involve an increase in S1P1 mRNA (Fig. 5*A*).

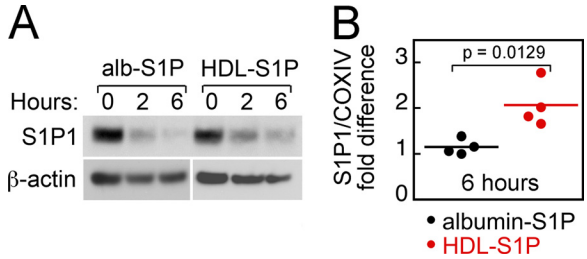

FIGURE 4. **HDP-S1P induces a less rapid decrease in levels of S1P1 than albumin-S1P.** *A*, anti-S1P1 immunoblot analysis of extracts from endothelial cells treated for 0, 2, or 6 h with albumin-S1P (*alb-S1P*) or HDL-S1P (each containing 150 nM S1P). As a loading control, filters were also probed with β-actin antiserum. *B*, densitometric analysis of immunoblots of extracts of endothelial cells treated for 6 h with albumin-S1P or HDL-S1P. The plotted values represent S1P1 protein levels in experimental replicates normalized using cytochrome oxidase-IV (*COXIV*) as a reference protein. Student's *t* test ($\alpha = 0.05$) showed that S1P1 levels were significantly higher ($p = 0.0129$) 6 h following HDL-S1P treatment as compared with albumin-S1P.

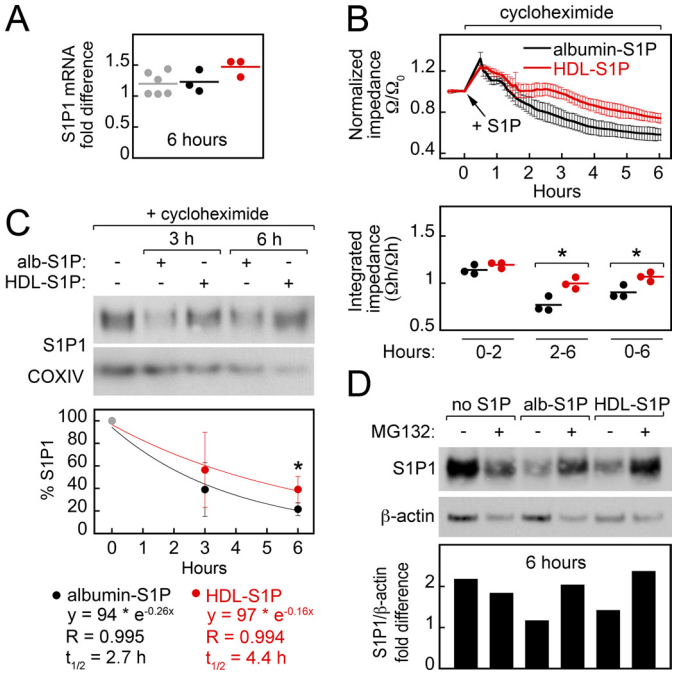

FIGURE 5. **HDL-S1P reduces the rate of S1P1 degradation as compared with albumin-S1P.** *A*, quantitative PCR analysis of S1P1 transcript levels in endothelial cells were treated with HDL-S1P, albumin-S1P (each containing 150 nM S1P), or S1P-free vehicle for 6 h. *B*, ECIS analysis of endothelial cells treated with cycloheximide (5 μg/ml) during treatments with either albumin-S1P or HDL-S1P (150 nM S1P). The *lower panel* shows integrated impedance values for the indicated time intervals. These values were obtained by dividing the integrated impedance values for each treatment by the mean integrated impedance values from cells treated with no S1P and no cycloheximide. Ω indicates ohms. *C*, immunoblot analysis of endothelial cells treated with cycloheximide (0.5 μg/ml) for 1 h and then up to 6 h with albumin-S1P (*alb-S1P*), HDL-S1P, or S1P-free vehicle. Diminishing levels of cytochrome oxidase-IV (*COXIV*) with time indicate the efficacy of cycloheximide at inhibiting *de novo* synthesis. S1P1 levels at 3 and 6 h were determined by densitometric analysis of immunoblots from four experiments as exemplified in the blot shown in *C*. Plotted values are the percentage of S1P1 in HDL-S1P-treated and albumin-S1P-treated cells relative to S1P1 levels in vehicle-treated controls (*gray*). The *p* value was determined using a one-sided Student's *t* test. *D*, anti-S1P1 immunoblot analysis of endothelial cells treated with albumin-S1P, HDL-S1P, or S1P-free vehicle ± the proteasome inhibitor MG132 (20 μM).

The possibility that the higher levels of S1P1 protein observed under conditions of HDL-S1P treatment were due to augmented protein synthesis were discounted by findings showing that the level of barrier enhancement by HDL-S1P remained greater than that of albumin-S1P under conditions of cycloheximide treatment (Fig. 5*B*).

HDL-S1P Reduces the Rate of S1P1 Degradation as Compared with Albumin-S1P—Hla and colleagues (30) have demonstrated that S1P induces S1P1 proteolysis via β-arrestin-mediated internalization, polyubiquitylation, and subsequent proteasomal degradation. To compare and contrast the effects of albumin-S1P *versus* HDL-S1P on S1P1 turnover, we first performed anti-S1P1 immunoblot analysis on extracts of endothelial cells treated for different periods of time with either HDL-S1P or albumin-S1P, under conditions of protein synthesis inhibition (Fig. 5*C*). Densitometric analysis of the anti-S1P1 reactive 45-kDa bands in four separate experiments was performed. Both albumin-S1P and HDL-S1P induced time-dependent decreases in S1P1 levels. The rate of S1P1 loss for each treatment was examined from the fits of the densitometric data to exponential functions. The results show that the reduction of S1P1 over time in response to HDL-S1P treatment is less than that occurring in response to albumin-S1P treatment ($p = 0.037$ at 6 h) (Fig. 5*C*). The half-life of S1P1 in response to HDL-S1P was 4.4 h as compared with 2.7 h in response to albumin-S1P.

We next evaluated the effect of proteasome inhibition on the loss of S1P1 in response to albumin-S1P and HDL-S1P treatments. Proteasomal inhibition was found to block all loss of S1P1 in response to HDL-S1P and albumin-S1P (Fig. 5*D*). Taken together, both HDL-S1P-induced degradation and albumin-S1P-induced S1P1 degradation are dependent on the proteasome; however, HDL-S1P induces less S1P1 degradation as compared with albumin-S1P.

Cell Surface Levels of S1P1 Are Higher after Treatment with HDL-S1P as Compared with Albumin-S1P—A number of studies have shown that S1P induces internalization of S1P1 (30–32). Thus, we were interested to know whether HDL-S1P and albumin-S1P differentially influenced cell surface levels of S1P1. Similar to what others have shown when using albumin-S1P (32), within 15 min of treatment with HDL-S1P, there is an apparent alteration in the subcellular distribution of the receptor (*i.e.* more discrete punctate staining) suggestive of internalization (Fig. 6*A*). In cells treated for 6 h, there was a greater degree of cell border and diffuse cellular S1P1 immunolabeling in HDL-S1P-treated *versus* albumin-S1P-treated cells (Fig. 6*B*) suggestive of differential effects on the cell surface localization of S1P1.

Using cell surface biotinylated endothelial cells, we found that levels of cell surface S1P1 were higher in endothelial cells after 3 h of treatment with HDL-S1P as compared with albumin-S1P (Fig. 6*C*). These findings, together with the evidence that HDL-S1P reduces degradation of S1P1 as compared with albumin-S1P, suggest that the sustained barrier effects of HDL-S1P may involve recycling of S1P1 to the cell surface. Indeed, when cells were treated with the recycling blocker, monensin, the long term barrier-promoting effects of HDL-S1P (*i.e.* >3.5 h) were abrogated ($p = 0.01$; Fig. 6, *D* and *E*). Thus, the contribution of S1P1 recycling to HDL-S1P enhanced barrier is apparent after the albumin-S1P effect on barrier is diminished (Fig. 1). Accordingly, it can be concluded that differences in

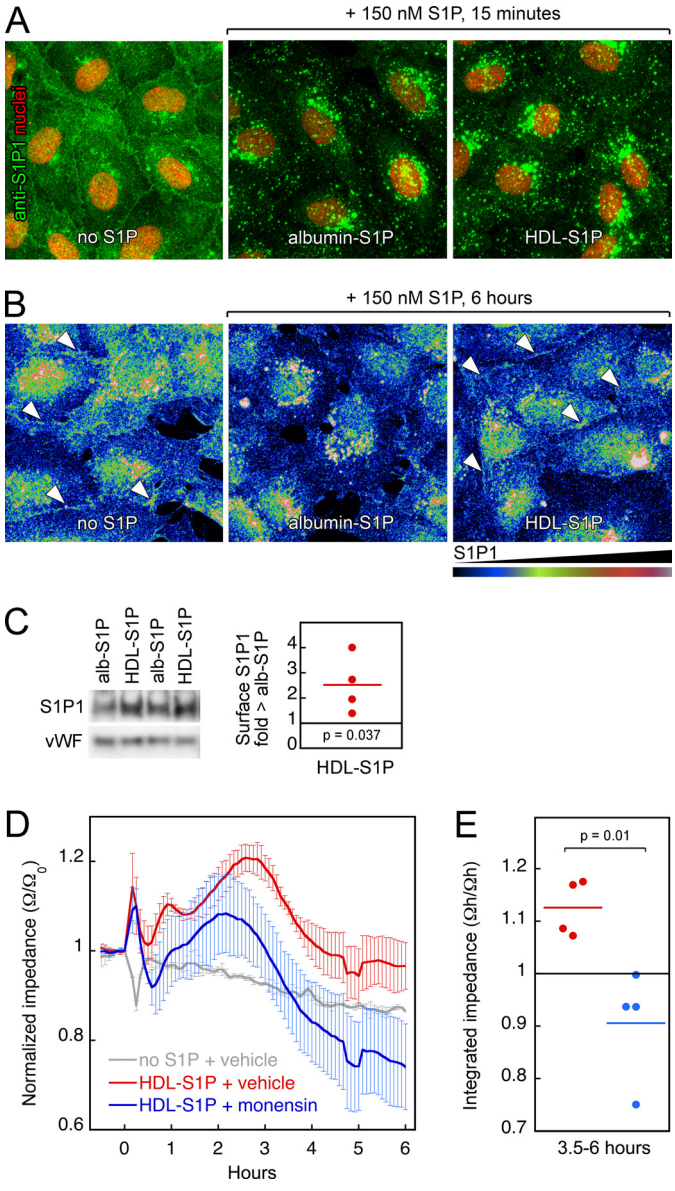

FIGURE 6. **Cell surface levels of S1P1 are higher after treatment with HDL-S1P as compared with albumin-S1P.** *A*, anti-S1P1 immunofluorescence analysis of endothelial cells treated for 15 min with HDL-S1P, albumin-S1P (each containing 150 nM S1P), or S1P-free vehicle. *B*, confocal immunofluorescence analysis of S1P1 in endothelial cells treated for 6 h with HDL-S1P, albumin-S1P (each containing 150 nM S1P), or S1P-free vehicle with a quantitative look-up table applied to the image. *Arrowheads* point to S1P1-rich cell borders. *C*, anti-S1P1 immunoblot analysis of biotinylated cell surface fractions from endothelial cells treated 3 h with HDL-S1P or albumin-S1P (each containing 150 nM S1P). Densitometric S1P1 values in each sample were normalized to the level of von Willebrand factor (*vWF*) and plotted to show fold differences in levels of surface S1P1 in HDL-S1P-treated cells relative to levels in albumin-S1P-treated cells. The plotted data contain values from two independent experiments. *p* was determined by one-sided, single group Student's *t* test compared against the value of 1. *D*, ECIS analysis of endothelial cells treated ± HDL-S1P in the presence of the G protein-coupled receptor recycling inhibitor monensin (285 nM) or vehicle. Ω indicates ohms. *E*, shows integrated impedance at the 3.5–6-h time interval after dividing mean integrated impedance values from cells treated with no S1P. The *p* value was determined by Student's *t* test.

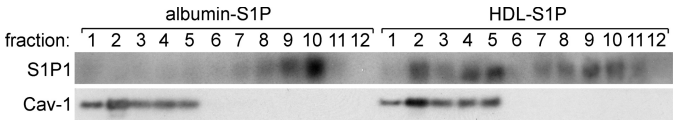

FIGURE 7. **HDL-S1P treatment increases S1P1 levels in caveolin-1-enriched microdomains as compared with albumin-S1P.** Following a 3-h treatment with HDL-S1P or albumin-S1P (each containing 150 nM S1P), extracts were made and subjected to density gradient ultracentrifugation. Fractions 1–12 were collected from top (lowest density) to bottom of the density gradient and subjected to immunoblot analysis using anti-S1P1 and anti-caveolin-1. Data are representative of two experiments.

S1P1 recycling underlie the disparate effects of HDL-S1P *versus* albumin-S1P on barrier.

HDL-S1P Induces Localization of S1P1 in Caveolin-enriched Microdomains—Because S1P-S1P1 signaling occurs within caveolin-enriched microdomains (CEMs) (6), we sought to determine whether HDL-S1P and albumin-S1P elicit differential effects on targeting of S1P1 to CEMs. We found that following 3 h of treatment with HDL-S1P, S1P1 was present in the CEM fractions, whereas there was little or no S1P1 detected in these fractions in response to albumin-S1P (Fig. 7).

DISCUSSION

Here we show that albumin-S1P and HDL-S1P have distinct effects on the persistence of S1P-dependent endothelial cell barrier enhancement such that HDL-S1P sustains endothelial cell barrier longer than albumin-S1P. Our findings indicate that HDL-S1P elicits specific effects on S1P1 trafficking that prolong S1P-S1P1 signaling involving persistent activation of Akt and eNOS. Consistently, we observed that the duration of the barrier promotion elicited by HDL-S1P lasted at least through 20 h after treatment (longer time points were not evaluated), whereas the barrier-promoting effects of albumin-S1P subsided within 4 h of treatment.

Previous studies established that both HDL-S1P and albumin-S1P stimulated relatively short duration activation of Erk1/2 and PI3K-Akt pathways as well as activation of eNOS (9, 13, 24). Here we showed that HDL-S1P but not albumin-S1P elicited a persistent activation of PI3K-Akt and eNOS, lasting for at least 6 h. By contrast, the duration of Erk1/2 activation stimulated by HDL-S1P treatment lasted less than 30 min. These findings together with evidence that inhibition of S1P1, PI3K-Akt, eNOS, or sGC blocked the sustained barrier effects elicited by HDL-S1P indicate that the HDL-S1P-S1P1-PI3K-Akt-eNOS-sGC pathway mediates sustained endothelial barrier activity. Furthermore, HDL-S1P augmented levels of total eNOS, whereas albumin-S1P had no effect on total eNOS levels, which is a means by which the flux through the pathway may be amplified. Our findings also highlight a new role of S1P1 signaling that involves its ability to maintain basal Erk1/2 and Akt levels.

Mechanistically, we also find that relative to albumin-S1P, HDL-S1P acts to reduce the rate of S1P1 protein degradation and promote recycling of internalized S1P1, leading to increased levels of the receptor on the endothelial cell surface. In addition to increasing cell surface S1P1 levels, HDL-S1P also acts to promote retention of S1P1 within CEMs, sites of S1P1 signaling (6). Previous studies have shown that within 5 min of S1P stimulation, S1P1 is recruited to CEMs (6). Our studies show that CEMs contain higher S1P1 levels 3 h after treatment with HDL-S1P as compared with treatment with albumin-S1P. Together, our findings suggest that enhanced S1P1 recycling underlies the sustaining effects of HDL-S1P on endothelial cell barrier. Although S1P1 recycling is known to be initiated in

response to S1P stimulation (31), the recycling process has not been fully defined. Protein kinase C activity (33) and *N*-glycosylation at the amino terminus of S1P1 (34, 35) are factors in S1P1 recycling, and our findings demonstrate that the type of S1P carrier is a key determinant in the process. Future studies will need to determine whether the differential effects of HDL and albumin on S1P1 are mediated by carrier-specific interactions with receptors and/or components of the endocytic apparatus.

The critical role of S1P in supporting vascular barrier integrity *in vivo* under basal conditions has been illustrated in animal models (36). The fact that both albumin-S1P and HDL-S1P are present in plasma leads to the question of their significance to S1P-dependent basal vascular barrier integrity. Our findings that exposure of endothelial monolayers to albumin-S1P alone leads to barrier permeability after 4 h, whereas HDL-S1P sustained long term barrier, suggest that the barrier-enhancing effects of HDL-S1P must predominate *in vivo*. Support for this comes from studies in which we observed long duration barrier enhancement when endothelial cells are treated with a combination of albumin-S1P and HDL-S1P (supplemental Fig. 3). In addition to HUVECs, we observe similar effects of HDL-S1P *versus* albumin-S1P on lung microvascular endothelial cells (supplemental Fig. 4).

Recent studies have demonstrated that apoM is the carrier of S1P in HDL (13, 37). ApoM-deficient mice lack HDL-associated S1P and display endothelial cell barrier dysfunction (*i.e.* increased vascular permeability under basal conditions). Vascular permeability occurs in apoM nulls despite the fact that their blood contains albumin-S1P levels similar to wild-type mice (13). Thus, in the absence of HDL-S1P, albumin-S1P is not able to fully maintain endothelial cell barrier function. This conclusion is in accordance with our findings showing that HDL-S1P has effects on the S1P1 signaling axis that are not shared with albumin-S1P.

In light of findings from the apoM mouse study and the present study, it can be inferred not only that S1P carried on HDL is responsible for regulating endothelial barrier homeostasis, but that physiological variation in HDL-S1P levels could have effects on the etiology of diseases associated with endothelial barrier dysfunction. Indeed, recent findings show that patients with increased endothelial permeability and edema resulting from cardiopulmonary bypass have a reduction in postoperative plasma levels of HDL (38). Furthermore, individuals with high levels of HDL and clinical evidence of heart disease have low levels of S1P in the HDL-containing fraction of serum (39). Thus, chronically low levels of HDL-S1P may contribute to both the etiology and the progression of atherosclerosis and be a biomarker for assessing risk in individuals with susceptibility to ischemic heart disease, yet lacking conventional risk factors such as elevated LDL-cholesterol or low HDL-cholesterol. This also raises the possibility that therapies that target HDL-S1P-mediated vascular effects may hold promise in treatment of ischemic heart disease and other vascular disorders with EC barrier dysfunction. Overall the findings suggest that continuing to define the functional properties of HDL-S1P may be key to deciphering the cardiovascular protective role of HDL.

REFERENCES

1. Mehta, D., and Malik, A. B. (2006) Signaling mechanisms regulating endothelial permeability. *Physiol. Rev.* **86,** 279–367
2. Dudek, S. M., and Garcia, J. G. (2001) Cytoskeletal regulation of pulmonary vascular permeability. *J. Appl. Physiol.* **91,** 1487–1500
3. Kumar, P., Shen, Q., Pivetti, C. D., Lee, E. S., Wu, M. H., and Yuan, S. Y. (2009) Molecular mechanisms of endothelial hyperpermeability: implications in inflammation. *Expert. Rev. Mol. Med.* **11,** e19
4. Garcia, J. G., Liu, F., Verin, A. D., Birukova, A., Dechert, M. A., Gerthoffer, W. T., Bamberg, J. R., and English, D. (2001) Sphingosine 1-phosphate promotes endothelial cell barrier integrity by Edg-dependent cytoskeletal rearrangement. *J. Clin. Invest.* **108,** 689–701
5. McVerry, B. J., and Garcia, J. G. (2005) *In vitro* and *in vivo* modulation of vascular barrier integrity by sphingosine 1-phosphate: mechanistic insights. *Cell. Signal.* **17,** 131–139
6. Singleton, P. A., Dudek, S. M., Chiang, E. T., and Garcia, J. G. (2005) Regulation of sphingosine 1-phosphate-induced endothelial cytoskeletal rearrangement and barrier enhancement by S1P1 receptor, PI3 kinase, Tiam1/Rac1, and α-actinin. *FASEB J.* **19,** 1646–1656
7. Sanchez, T., Skoura, A., Wu, M. T., Casserly, B., Harrington, E. O., and Hla, T. (2007) Induction of vascular permeability by the sphingosine-1-phosphate receptor-2 (S1P2R) and its downstream effectors ROCK and PTEN. *Arterioscler. Thromb. Vasc. Biol.* **27,** 1312–1318
8. Xu, M., Waters, C. L., Hu, C., Wysolmerski, R. B., Vincent, P. A., and Minnear, F. L. (2007) Sphingosine 1-phosphate rapidly increases endothelial barrier function independently of VE-cadherin but requires cell spreading and Rho kinase. *Am. J. Physiol. Cell Physiol.* **293,** C1309–C1318
9. Argraves, K. M., Gazzolo, P. J., Groh, E. M., Wilkerson, B. A., Matsuura, B. S., Twal, W. O., Hammad, S. M., and Argraves, W. S. (2008) High density lipoprotein-associated sphingosine 1-phosphate promotes endothelial barrier function. *J. Biol. Chem.* **283,** 25074–25081
10. Lee, J. F., Gordon, S., Estrada, R., Wang, L., Siow, D. L., Wattenberg, B. W., Lominadze, D., and Lee, M. J. (2009) Balance of S1P1 and S1P2 signaling regulates peripheral microvascular permeability in rat cremaster muscle vasculature. *Am. J. Physiol. Heart Circ. Physiol.* **296,** H33–H42
11. Sarai, K., Shikata, K., Shikata, Y., Omori, K., Watanabe, N., Sasaki, M., Nishishita, S., Wada, J., Goda, N., Kataoka, N., and Makino, H. (2009) Endothelial barrier protection by FTY720 under hyperglycemic condition: involvement of focal adhesion kinase, small GTPases, and adherens junction proteins. *Am. J. Physiol. Cell Physiol.* **297,** C945–C954
12. Zhang, G., Xu, S., Qian, Y., and He, P. (2010) Sphingosine-1-phosphate prevents permeability increases via activation of endothelial sphingosine-1-phosphate receptor 1 in rat venules. *Am. J. Physiol. Heart Circ. Physiol.* **299,** H1494–H1504
13. Christoffersen, C., Obinata, H., Kumaraswamy, S. B., Galvani, S., Ahnström, J., Sevvana, M., Egerer-Sieber, C., Muller, Y. A., Hla, T., Nielsen, L. B., and Dahlbäck, B. (2011) Endothelium-protective sphingosine-1-phosphate provided by HDL-associated apolipoprotein M. *Proc. Natl. Acad. Sci. U.S.A.* **108,** 9613–9618
14. Murata, N., Sato, K., Kon, J., Tomura, H., Yanagita, M., Kuwabara, A., Ui, M., and Okajima, F. (2000) Interaction of sphingosine 1-phosphate with plasma components, including lipoproteins, regulates the lipid receptor-mediated actions. *Biochem. J.* **352,** 809–815
15. Bielawski, J., Szulc, Z. M., Hannun, Y. A., and Bielawska, A. (2006) Simultaneous quantitative analysis of bioactive sphingolipids by high-performance liquid chromatography-tandem mass spectrometry. *Methods* **39,** 82–91
16. Wasan, K. M., Cassidy, S. M., Kennedy, A. L., and Peteherych, K. D. (2000) Lipoprotein isolation and analysis from serum by preparative ultracentrifugation. in *Atherosclerosis: Experimental Methods and Protocols* (Drew, A. F. ed), pp. 27–35, Humana Press, Totowa, NJ
17. Oliferenko, S., Paiha, K., Harder, T., Gerke, V., Schwärzler, C., Schwarz, H., Beug, H., Günthert, U., and Huber, L. A. (1999) Analysis of CD44-containing lipid rafts: Recruitment of annexin II and stabilization by the actin cytoskeleton. *J. Cell Biol.* **146,** 843–854
18. Thankamony, S. P., and Knudson, W. (2006) Acylation of CD44 and its association with lipid rafts are required for receptor and hyaluronan en-

docytosis. *J. Biol. Chem.* **281,** 34601–34609
19. Zuker, M. (2003) Mfold web server for nucleic acid folding and hybridization prediction. *Nucleic Acids Res.* **31,** 3406–3415
20. Rozen, S., and Skaletsky, H. (2000) Primer3 on the WWW for general users and for biologist programmers. *Methods Mol. Biol.* **132,** 365–386
21. Zhao, S., and Fernald, R. D. (2005) Comprehensive algorithm for quantitative real-time polymerase chain reaction. *J. Comput. Biol.* **12,** 1047–1064
22. Pfaffl, M. W. (2001) A new mathematical model for relative quantification in real-time RT-PCR. *Nucleic Acids Res.* **29,** e45
23. Whetzel, A. M., Bolick, D. T., and Hedrick, C. C. (2009) Sphingosine-1-phosphate inhibits high glucose-mediated ERK1/2 action in endothelium through induction of MAP kinase phosphatase-3. *Am. J. Physiol. Cell Physiol.* **296,** C339–C345
24. Nofer, J. R., van der Giet, M., Tölle, M., Wolinska, I., von Wnuck Lipinski, K., Baba, H. A., Tietge, U. J., Gödecke, A., Ishii, I., Kleuser, B., Schäfers, M., Fobker, M., Zidek, W., Assmann, G., Chun, J., and Levkau, B. (2004) HDL induces NO-dependent vasorelaxation via the lysophospholipid receptor S1P3. *J. Clin. Invest.* **113,** 569–581
25. Peng, X. Q., Damarla, M., Skirball, J., Nonas, S., Wang, X. Y., Han, E. J., Hasan, E. J., Cao, X., Boueiz, A., Damico, R., Tuder, R. M., Sciuto, A. M., Anderson, D. R., Garcia, J. G., Kass, D. A., Hassoun, P. M., and Zhang, J. T. (2010) Protective role of PI3-kinase/Akt/eNOS signaling in mechanical stress through inhibition of p38 mitogen-activated protein kinase in mouse lung. *Acta Pharmacol. Sin.* **31,** 175–183
26. May, J. M., and Qu, Z. C. (2011) Nitric oxide mediates tightening of the endothelial barrier by ascorbic acid. *Biochem. Biophys. Res. Commun.* **404,** 701–705
27. Rämet, M. E., Rämet, M., Lu, Q., Nickerson, M., Savolainen, M. J., Malzone, A., and Karas, R. H. (2003) High-density lipoprotein increases the abundance of eNOS protein in human vascular endothelial cells by increasing its half-life. *J. Am. Coll. Cardiol.* **41,** 2288–2297
28. Gündüz, D., Thom, J., Hussain, I., Lopez, D., Härtel, F. V., Erdogan, A., Grebe, M., Sedding, D., Piper, H. M., Tillmanns, H., Noll, T., and Aslam, M. (2010) Insulin stabilizes microvascular endothelial barrier function via phosphatidylinositol 3-kinase/Akt-mediated Rac1 activation. *Arterioscler. Thromb. Vasc. Biol.* **30,** 1237–1245
29. Oo, M. L., Chang, S. H., Thangada, S., Wu, M. T., Rezaul, K., Blaho, V., Hwang, S. I., Han, D. K., and Hla, T. (2011) Engagement of $S1P_1$-degradative mechanisms leads to vascular leak in mice. *J. Clin. Invest.* **121,** 2290–2300
30. Oo, M. L., Thangada, S., Wu, M. T., Liu, C. H., Macdonald, T. L., Lynch, K. R., Lin, C. Y., and Hla, T. (2007) Immunosuppressive and anti-angiogenic sphingosine 1-phosphate receptor-1 agonists induce ubiquitinylation and proteasomal degradation of the receptor. *J. Biol. Chem.* **282,** 9082–9089
31. Liu, C. H., Thangada, S., Lee, M. J., Van Brocklyn, J. R., Spiegel, S., and Hla, T. (1999) Ligand-induced trafficking of the sphingosine-1-phosphate receptor EDG-1. *Mol. Biol. Cell* **10,** 1179–1190
32. Mullershausen, F., Zecri, F., Cetin, C., Billich, A., Guerini, D., and Seuwen, K. (2009) Persistent signaling induced by FTY720-phosphate is mediated by internalized S1P1 receptors. *Nat. Chem. Biol.* **5,** 428–434
33. Sensken, S. C., and Gräler, M. H. (2010) Down-regulation of S1P1 receptor surface expression by protein kinase C inhibition. *J. Biol. Chem.* **285,** 6298–6307
34. Kohno, T., and Igarashi, Y. (2003) Truncation of the N-terminal ectodomain has implications in the *N*-glycosylation and transport to the cell surface of Edg-1/S1P1 receptor. *J. Biochem.* **134,** 667–673
35. Kohno, T., Wada, A., and Igarashi, Y. (2002) *N*-Glycans of sphingosine 1-phosphate receptor Edg-1 regulate ligand-induced receptor internalization. *FASEB J.* **16,** 983–992
36. Li, X., Stankovic, M., Bonder, C. S., Hahn, C. N., Parsons, M., Pitson, S. M., Xia, P., Proia, R. L., Vadas, M. A., and Gamble, J. R. (2008) Basal and angiopoietin-1-mediated endothelial permeability is regulated by sphingosine kinase-1. *Blood* **111,** 3489–3497
37. Karuna, R., Park, R., Othman, A., Holleboom, A. G., Motazacker, M. M., Sutter, I., Kuivenhoven, J. A., Rohrer, L., Matile, H., Hornemann, T., Stoffel, M., Rentsch, K. M., and von Eckardstein, A. (2011) Plasma levels of sphingosine-1-phosphate and apolipoprotein M in patients with monogenic disorders of HDL metabolism. *Atherosclerosis* **219,** 855–863
38. Zyblewski, S. C., Argraves, W. S., Graham, E. M., Slate, E. H., Atz, A. M., Bradley, S. M., McQuinn, T. C., Wilkerson, B. A., Wing, S. B., and Argraves, K. M. (2012) Reduction in postoperative high-density lipoprotein cholesterol levels in children undergoing the Fontan operation. *Pediatr Cardiol.* **33,** 1154–1159
39. Argraves, K. M., Sethi, A. A., Gazzolo, P. J., Wilkerson, B. A., Remaley, A. T., Tybjaerg-Hansen, A., Nordestgaard, B. G., Yeatts, S. D., Nicholas, K. S., Barth, J. L., and Argraves, W. S. (2011) S1P, dihydro-S1P, and C24: 1-ceramide levels in the HDL-containing fraction of serum inversely correlate with occurrence of ischemic heart disease. *Lipids Health Dis.* **10,** 70